© 2014. Published by The Company of Biologists Ltd | Development (2014) 141, 1821-1834 doi:10.1242/dev.103242

RESEARCH ARTICLE

STEM CELLS AND REGENERATION

Hemogenic endothelium generates mesoangioblasts that contribute to several mesodermal lineages *in vivo*

Emanuele Azzoni[1,2,*], Valentina Conti[1,2], Lara Campana[2], Arianna Dellavalle[2], Ralf H. Adams[3,4], Giulio Cossu[2,5] and Silvia Brunelli[1,2,‡]

ABSTRACT

The embryonic endothelium is a known source of hematopoietic stem cells. Moreover, vessel-associated progenitors/stem cells with multilineage mesodermal differentiation potential, such as the 'embryonic mesoangioblasts', originate *in vitro* from the endothelium. Using a genetic lineage tracing approach, we show that early extra-embryonic endothelium generates, in a narrow time-window and prior to the hemogenic endothelium in the major embryonic arteries, hematopoietic cells that migrate to the embryo proper, and are subsequently found within the mesenchyme. A subpopulation of these cells, distinct from embryonic macrophages, co-expresses mesenchymal and hematopoietic markers. In addition, hemogenic endothelium-derived cells contribute to skeletal and smooth muscle, and to other mesodermal cells *in vivo*, and display features of embryonic mesoangioblasts *in vitro*. Therefore, we provide new insights on the distinctive characteristics of the extra-embryonic and embryonic hemogenic endothelium, and we identify the putative *in vivo* counterpart of embryonic mesoangioblasts, suggesting their identity and developmental ontogeny.

KEY WORDS: VE-Cadherin, Hemogenic endothelium, Mesoangioblasts, Muscle, Mouse

INTRODUCTION

The vascular and the hematopoietic systems are deeply entwined throughout embryonic development. The first endothelial cells (ECs) in the gastrulating embryo originate from the lateral and posterior mesoderm. Later, they migrate towards the yolk sac (YS), where they differentiate into ECs and hematopoietic cells (HCs) of the blood islands (Medvinsky et al., 2011). This close anatomical and temporal relationship between HCs and ECs has suggested a shared common mesodermal ancestor: the hemangioblast. This progenitor was initially identified in the embryonic stem cell (ESC) model (Yamashita et al., 2000). Other studies associate the first hematopoietic stem cells (HSCs) with phenotypically differentiated ECs endowed with hematopoietic potential: the hemogenic endothelium. Indeed, fate-mapping and *in vivo* time-lapse imaging in mouse and zebrafish revealed that HCs originate from VE-Cadherin$^+$ (VE-Cad, *Cdh5*) ECs in the dorsal aorta (Bertrand et al., 2010; Boisset et al., 2010; Kissa and Herbomel, 2010; Zovein et al., 2008) and insights have also been given on the different potential of hemogenic endothelial progenitors (Chen et al., 2011). By linking these two hypotheses, it has been demonstrated in the ESC model that the hemangioblast generates HCs through the formation of a hemogenic endothelium intermediate. This cell population is found in gastrulating mouse embryos and generates HCs on further culture (Lancrin et al., 2009).

The embryonic dorsal aorta is the source of another population of progenitor cells, named mesoangioblasts (MABs) (Minasi et al., 2002). These culture-defined cells express hemangioblastic, hematopoietic, endothelial and mesodermal markers, and possess self-renewal capacity and mesodermal differentiation potency *in vitro* and *in vivo* (Brunelli et al., 2004; Minasi et al., 2002); *in vitro* only, they display hematopoietic potential. MABs have been successfully used in cell transplantation protocols that led to a significant recovery of the structure and function of skeletal muscle in dystrophic animals (Brunelli et al., 2007; Sampaolesi et al., 2003). Although MAB myogenic potency is certainly useful for cell transplantation protocols, no insights have been obtained on their origin, role during normal development and tissue remodeling, or their relationship with other postnatal vessel-associated cells with therapeutic potential (Dellavalle et al., 2011; Mitchell et al., 2010).

To follow the fate of VE-Cad expressing ECs in the early and late embryo, we performed a genetic lineage-tracing analysis, combining pulses of induction of Cre recombinase with a time course evaluation of the reporter expression. We show that extra-embryonic VE-Cad$^+$ endothelium generates the first wave of HCs that colonize the embryo mesenchyme. Moreover, we identify hemogenic endothelium as the source of progenitor cells that resemble embryonic MABs and physiologically contribute to several mesodermal lineages in the embryo, including skeletal muscle.

RESULTS

The Cdh5-CreER^{T2} line leads to efficient and endothelial specific Cre recombination in the embryo

To genetically label endothelial-derived cell populations, we used the Cdh5-CreER^{T2} transgenic mouse (Wang et al., 2010), expressing a tamoxifen (TAM)-inducible form of Cre recombinase (CRE-ER^{T2}) under the control of VE-Cad regulatory sequences. All experiments were performed in Cdh5-CreER^{T2};R26R-EYFP (Srinivas et al., 2001) double transgenics.

We induced Cre recombination with one single intraperitoneal (I/P) TAM injection in the pregnant mother at E8.5 (Fig. 1A) to avoid labeling the YS mesoderm, which transiently expresses VE-Cad at E7.5 (Drake and Fleming, 2000). FACS analysis of cells dissociated from E9.5 embryos showed a higher percentage of EYFP$^+$ cells in the YS, followed by placenta and embryo proper (Fig. 1B). The efficiency of Cre recombination was first measured by FACS as the percentage of EYFP$^+$ cells in the CD31$^+$ population, and was found to be 65.1±4.7% in the embryo proper 24 h after Cre induction

[1]Department of Health Sciences, University of Milano-Bicocca, Monza 20900, Italy. [2]San Raffaele Scientific Institute, Division of Regenerative Medicine, Stem Cells and Gene Therapy, Via Olgettina 58, Milan 20132, Italy. [3]Max Planck Institute for Molecular Biomedicine, Department of Tissue Morphogenesis, Münster D-48149, Germany. [4]University of Münster, Faculty of Medicine, Münster D-48149, Germany. [5]Institute of Inflammation and Repair, University of Manchester, Manchester M13 9PL, UK.
*Present address: MRC Molecular Haematology Unit, Weatherall Institute of Molecular Medicine, Oxford OX3 9DS, UK.

‡Author for correspondence (brunelli.silvia@hsr.it)

Received 30 August 2013; Accepted 12 March 2014

Development (2014) 141, 1821-1834 doi:10.1242/dev.103242

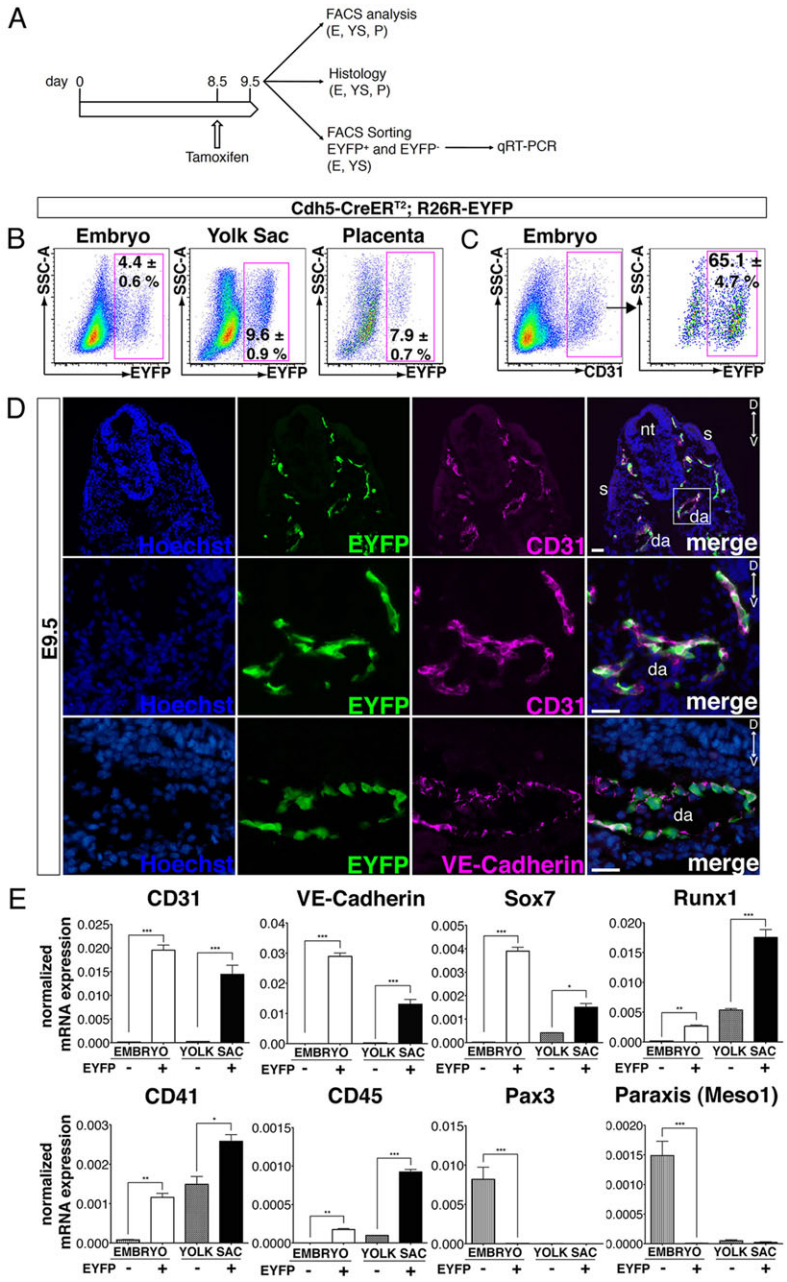

Fig. 1. Efficiency and specificity of Cre recombination in Cdh5-CREER^{T2}; R26R-EYFP double transgenic mice. (A) Experimental scheme. (B,C) FACS analysis showing (B) the percentage of EYFP$^+$ cells and (C) Cre recombination efficiency. (D) Immunofluorescence (IF) using anti-EYFP-, anti-CD31- and anti-VE-Cad-specific antibodies on transverse sections of E9.5 embryos. Nuclei were stained with Hoechst. Dorsoventral orientation is shown. da, dorsal aorta; nt, neural tube; s, somite. Scale bars: 50 μm. (E) qRT-PCR analysis. Data points were calculated as gene expression relative to cyclophilin A (CD31, VE-Cadherin, Sox7, Runx1, CD41 and CD45) or 28S (Pax3 and Paraxis). Data are mean±s.e.m.; n=3 independent experiments. *P<0.05; **P<0.01; ***P<0.001.

(Fig. 1C). Immunofluorescence (IF) analysis of E9.5 embryos revealed co-localization of EYFP with endothelial-specific markers (VE-Cad and CD31/Pecam1) (Fig. 1D). Cre recombination efficiency (estimated as the number of EYFP$^+$ cells on total CD31$^+$ or VE-Cadherin$^+$ cells) was approximately 80% (Fig. 1D). At this stage, EYFP$^+$CD31$^-$ or EYFP$^+$VE-Cad$^-$ cells were undetectable in the embryo proper. As a control of Cre recombination leakage, we performed IF and FACS analysis on embryos without TAM induction. At all stages analyzed (E10.5-E15.5), we occasionally detected very rare EYFP$^+$ cells (in one-quarter of analyzed samples, 0.01% of the total cells in the embryo). These were invariably CD31$^+$ and/or VE-Cadherin$^+$ (supplementary material Fig. S1A-C). This minimal amount of Cre leakage was accounted for; nevertheless, it did not affect the conclusions of our study.

Strict tissue specificity is a crucial issue for all lineage-tracing approaches. To verify this, TAM injection was performed at E8.5, and EYFP$^+$ and EYFP$^-$ cells were separately sorted from the embryo proper and the YS at E9.5 (gating as in Fig. 1B). qRT-PCR analysis showed that *Pax3* (paraxial mesoderm, dermamyotome) and *paraxis* (paraxial mesoderm) mRNAs were confined in the EYFP$^-$ population (Fig. 1E). VE-Cad and CD31-expressing cells were found almost entirely in the EYFP$^+$ fraction in both embryo proper and YS, further confirming the recombination efficiency. *Runx1* (hemogenic ECs and HCs) was mainly expressed in the YS, and also in EYFP$^-$ cells, as were CD41 (*Itga2b*) and CD45 (*Ptprc*) (other markers of HCs). *Sox7*, a gene found to regulate VE-Cad expression in the hemogenic endothelium (Costa et al., 2012) was exclusively expressed in EYFP$^+$ cells in the embryo, while it was detected in both EYFP$^+$ and EYFP$^-$ cells in the YS. These results confirmed that induction of Cre recombination at E8.5 resulted in labeling of cells that express VE-Cad (eVE-Cad$^+$ for embryonic VE-Cadherin-expressing cells), have mainly an endothelial phenotype in the embryo and also a hematopoietic phenotype in the YS, while completely lacking paraxial mesoderm characteristics.

Development (2014) 141, 1821-1834 doi:10.1242/dev.103242

Non-macrophage eVE-Cad$^+$-derived hematopoietic cells are found within the embryonic mesenchyme

The presence of abundant hematopoietic and hemogenic endothelium specific transcripts 24 h after induction in eVE-Cad$^+$-derived cells prompted us to investigate their hematopoietic nature and fate. The endothelium in the embryo proper contributes to definitive hematopoiesis (Boisset et al., 2010; Zovein et al., 2008), starting at E10-E10.5 in the dorsal aorta, with rare clusters appearing in the umbilical and vitelline arteries at E9.5 (Yokomizo et al., 2011). Indeed, at E10.5-E11.5, we detected EYFP$^+$ intra-aortic clusters originating from EYFP$^+$CD31$^+$ hemogenic endothelium (supplementary material Fig. S2). All EYFP$^+$ intra-aortic cluster cells expressed Kit. Most clusters were CD31$^+$ and also expressed CD41 or CD45 (supplementary material Fig. S2).

Conversely, at E9.5 only rare EYFP$^+$ cells in the embryo proper expressed hematopoietic markers (Fig. 2A,D,E), whereas EYFP$^+$CD45$^+$ and EYFP$^+$CD41$^+$ cells were found in the YS (Fig. 2B,D-E) and less abundantly in the placenta (Fig. 2C-E). We detected EYFP$^+$Kit$^+$ cells in the YS as early as E9 (supplementary material Fig. S3i-ii). This implies that the YS endothelium, and to a lesser extent the placental endothelium, are already hemogenic at E8.5.

Further IF analysis in the placenta revealed the presence of EYFP$^+$CD45$^+$ and EYFP$^+$CD41$^+$ cells at E10.5-E12.5 (supplementary material Fig. S4A). FACS analysis showed that among CD45$^+$ cells, EYFP$^+$ cells accounted for a lower percentage (1-2.5%) compared with YS and embryo (20-30%) (supplementary material Fig. S4B). Considering that many placental CD45$^+$ cells are of maternal origin, and thus EYFP$^-$, these data suggest that a small, but still significant, number of hematopoietic cells in the placenta are of endothelial origin.

We then focused on the fate of EYFP$^+$ cells in the embryo proper, from E10.5 (Fig. 3A). In addition to endothelial and intra-aortic hematopoietic clusters, EYFP$^+$CD45$^+$ cells could be seen on the abluminal side of vessels and in the surrounding mesenchyme (Fig. 3B-Ci). This was evident around the dorsal aorta (arrows in Fig. 3B-Ci; supplementary material Movie 1) and around vessels in the limb bud (arrow in supplementary material Fig. S5Ai). Some EYFP$^+$CD41$^+$ cells were also observed in the mesenchyme (supplementary material Fig. S5Aii). At E10.5, the number of EYFP$^+$CD41$^+$ and EYFP$^+$CD45$^+$ cells in the mesenchyme of the embryo proper was almost equivalent (Fig. 3D); some of them expressed Kit$^+$ (supplementary material Fig. S3iii-iv). CD45$^+$ cells in the mesenchyme were not natively labeled as they did not express endothelial markers (Fig. 3B-Ci; supplementary material Fig. S5Ai), which means labeling must have occurred at an earlier time. Moreover, at E10.5 these were the only EYFP$^+$VE-Cad$^-$ cells in the embryo. At E11.5 a higher number of EYFP$^+$CD45$^+$CD31$^-$ cells were present in the mesenchyme, in particular in the subaortic mesenchyme (Fig. 3Cii,D; supplementary material Movie 2 and Fig. S5Aiii). EYFP$^+$CD41$^+$ cells and EYFP$^+$Kit$^+$ cells were also detected in the

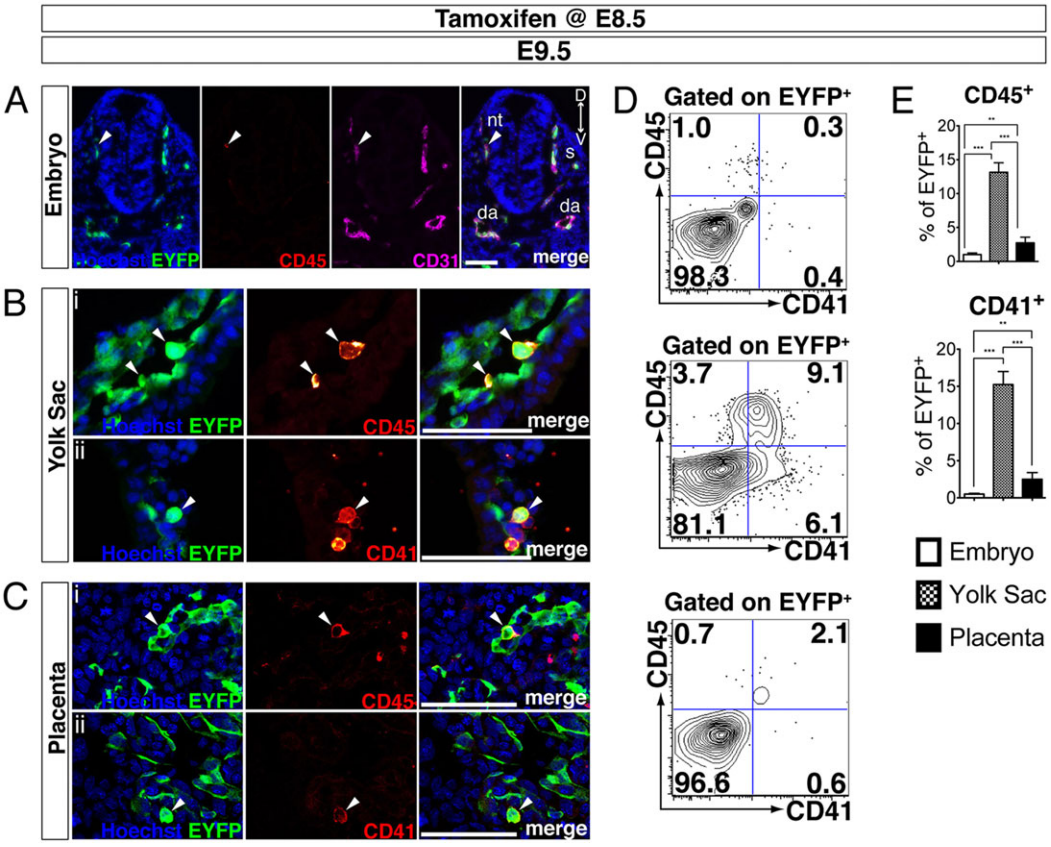

Fig. 2. eVE-Cad$^+$-derived cells in extra-embryonic tissues generate hematopoietic cells (HCs) at early stages. (A) Immunofluorescence (IF) using anti-EYFP, anti-CD31 and anti-CD45 on transverse sections of a E9.5 embryo. Arrowheads indicate an unlabeled CD45$^+$CD31$^+$ HC. Dorsoventral orientation is shown. (B,C) IF using anti-EYFP and anti-CD45 (i) or anti-CD41 (ii) on sections of E9.5 YS (B) or placenta (C). Arrowheads indicate EYFP$^+$CD45$^+$ or EYFP$^+$CD41$^+$ HCs. Nuclei were stained with Hoechst. Scale bars: 50 μm. (D) FACS analysis showing the percentage of CD41$^+$ and CD45$^+$ cells within the EYFP$^+$ subset in embryos (upper panel), YS (mid panel) and placenta (lower panel). Dot plots are representative of at least three independent experiments. (E) Graph showing the percentage of CD45$^+$ and CD41$^+$ cells within the EYFP$^+$ subset as quantification of FACS analyses. Data are mean±s.e.m. $^{**}P<0.01$; $^{***}P<0.001$.

Development (2014) 141, 1821-1834 doi:10.1242/dev.103242

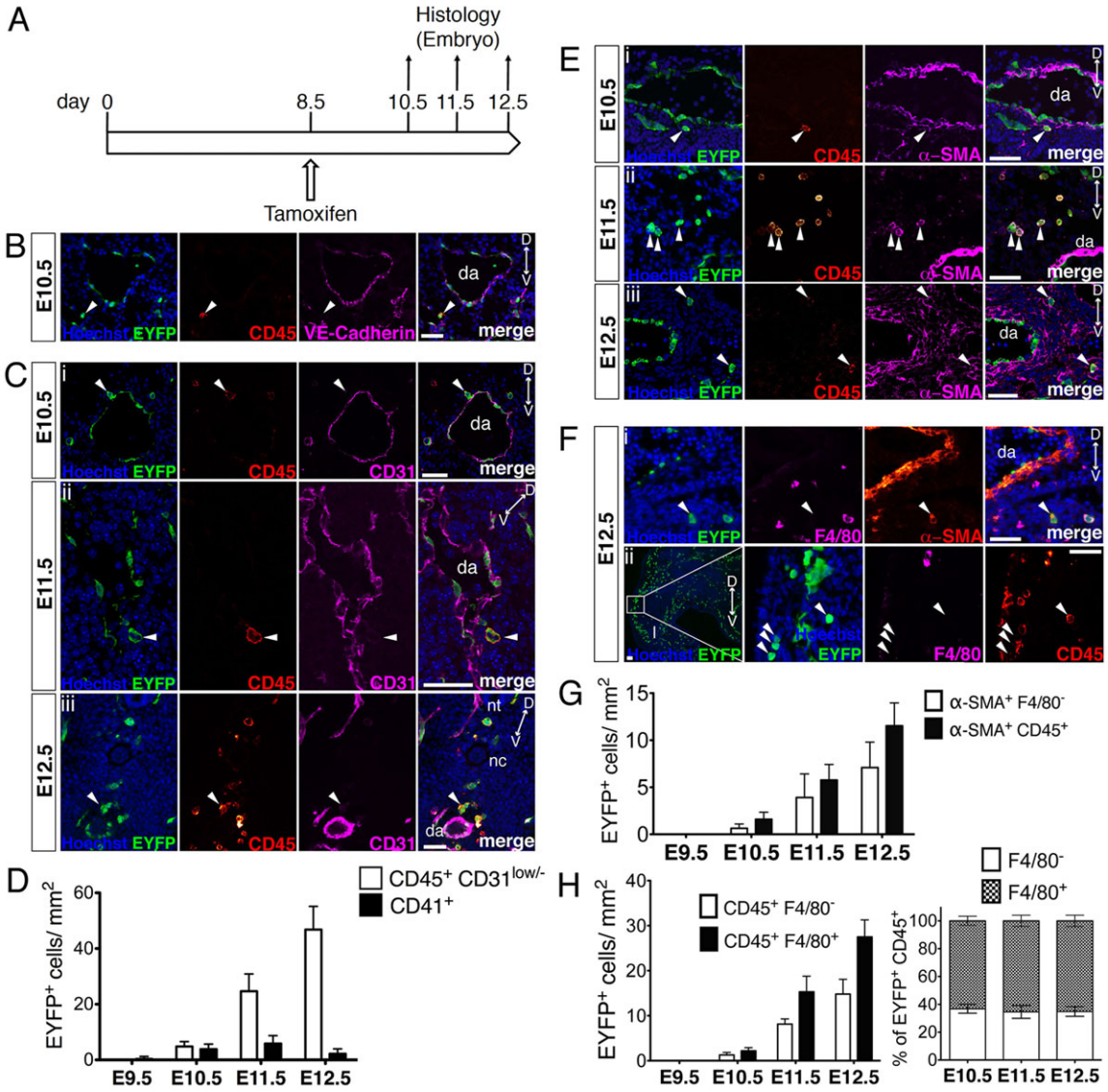

Fig. 3. eVE-Cad$^+$-derived non-MΦ HCs emerge from vessels in an abluminal direction and express the mesenchymal marker α-SMA. (A) Experimental scheme. (B) Immunofluorescence (IF) using anti-EYFP, anti-CD45 and anti-VE-Cadherin on transverse sections of a E10.5 embryo. Arrowheads indicate a EYFP$^+$CD45$^+$VE-Cadherin$^-$ cell in the subaortic mesenchyme. (C) IF using anti-EYFP, anti-CD45 and anti-CD31 on transverse sections of E10.5 (i), E11.5 (ii) and E12.5 (iii) embryos. Arrowheads indicate abluminal EYFP$^+$CD45$^+$CD31$^{low/-}$ cells. (D) Histological quantification of EYFP$^+$CD45$^+$CD31$^{low/-}$ and EYFP$^+$CD41$^+$ cells in the embryo mesenchyme. (E) IF using anti-EYFP, anti-CD45 and anti α-SMA on transverse sections of E10.5 (i), E11.5 (ii) and E12.5 (iii) embryos. Arrowheads indicate EYFP$^+$CD45$^+$α-SMA$^+$ cells in the mesenchyme surrounding dorsal aorta. (F) IF using anti-EYFP, anti-F4/80 and anti-α-SMA (i) or anti-CD45 (ii) on transverse sections of E12.5 embryos. Arrowheads indicate EYFP$^+$α-SMA$^+$F4/80$^-$ cells in the subaortic mesenchyme (i) and EYFP$^+$CD45$^+$F4/80$^-$ cells in the developing limb (ii). Nuclei were stained with Hoechst. Dorsoventral orientation is shown. Scale bars: 50 μm. da, dorsal aorta; l, limb. (G) Histological quantification of EYFP$^+$α-SMA$^+$ F4/80$^-$ and EYFP$^+$α-SMA$^+$CD45$^+$ cells in the embryo mesenchyme. (H) Histological quantification of EYFP$^+$CD45$^+$F4/80$^-$ and EYFP$^+$CD45$^+$F4/80$^+$ cells in the embryo mesenchyme. Left: absolute numbers; right: percentage of F4/80$^+$ and F4/80$^-$ cells on total EYFP$^+$CD45$^+$ cells.

embryo proper, outside EYFP$^+$CD31$^+$ vessels (supplementary material Fig. S3v-vi and Fig. S5Aiv). At E12.5, EYFP$^+$CD45$^+$ cells in the mesenchyme were even more abundant and could be detected throughout the whole embryo (Fig. 3Ciii,D; supplementary material Fig. S5B). At this stage, EYFP$^+$CD41$^+$ cells were rare in the mesenchyme (Fig. 3D). These data indicate that eVE-Cad$^+$ cells give rise to HCs that migrate into and through mesenchymal tissues.

Remarkably, at E10.5-E12.5 many isolated EYFP$^+$CD45$^+$ cells in the embryo mesenchyme also expressed α-SMA, which at these early stages is expressed in a range of cells of mesodermal origin (smooth, skeletal, cardiac muscle cells, pericytes) (Crawford et al., 2002) but not in HCs (Fig. 3Ei-iii,G). Primitive embryonic macrophages (MΦs) arise in the yolk sac as early as E7.5, before the appearance of definitive HSCs. Although they differ from adult MΦs, they are characterized by the unambiguous expression of markers such as F4/80 and CD11b (Bertrand et al., 2005; Ovchinnikov, 2008). A substantial percentage of EYFP$^+$CD45$^+$ cells in the mesenchyme were indeed F4/80$^+$ (Fig. 3Fi-ii,H). Still, from E10.5 to E12.5 about 35% of EYFP$^+$CD45$^+$ cells in the mesenchyme were not macrophages (F4/80$^-$) (Fig. 3Fii,H).

EYFP$^+$CD45$^+$α-SMA$^+$ and EYFP$^+$α-SMA$^+$F4/80$^-$ cells in the mesenchyme were detected in various anatomical locations, mostly associated perivascularly with large vessels (Fig. 3E,Fi) and in the developing limbs. These cells increased over time, their

Development (2014) 141, 1821-1834 doi:10.1242/dev.103242

ratio was similar (Fig. 3G) and they were invariably CD41$^-$ (supplementary material Fig. S5Aii,iv). At E12.5, about 52% of CD45$^+$α-SMA$^+$ F4/80$^-$ cells were EYFP$^+$ (supplementary material Fig. S5D; Table 1).

To further characterize eVE-Cad$^+$-derived cells in the embryo, we performed several analyses on freshly isolated cells. In particular, we focused on three different EYFP$^+$ cell subsets: CD45$^-$CD11b$^-$F4/80$^-$, CD45$^+$CD11b$^+$/F4/80$^+$ and CD45$^+$CD11b$^-$F4/80$^-$ (Fig. 4A,B). Sorting CD11b$^+$ and/or F4/80$^+$ cells ensures a high likelihood of inclusion of all macrophages (Pucci et al., 2009; Schulz et al., 2012); therefore, we will from now on refer to CD45$^+$CD11b$^+$/F4/80$^+$ cells as CD45$^+$MΦ, and to CD45$^+$CD11b$^-$F4/80$^-$ as CD45$^+$non-MΦ.

We characterized the above-mentioned populations by FACS and qRT-PCR on sorted fractions. At E12.5, CD45$^+$non-MΦ cells expressed high levels of markers for both HCs (Kit, CD41) and mesenchymal cells (CD73, CD71, α-SMA, PDGFR-β, endoglin/CD105) (Fig. 4C-E). CD45$^-$ cells expressed high levels of endothelial markers such as CD31, VE-Cadherin, Flk1, Tie2 and CD105. CD45$^+$MΦ were the only cells to express macrophage/myeloid-specific genes such as *Cx3Cr1* and PU.1 (*Spi1*). The latter also expressed other mesenchymal markers, but to a lesser extent compared with the CD45$^+$non-MΦ population, in particular at the protein level. Some of the CD45$^+$MΦ-expressing mesenchymal markers could be MΦs that have phagocytized mesenchymal cells and transiently acquired or exposed their antigens (Russo et al., 2000). However, as CD45$^+$MΦ also transcribe these genes, this is the first indication that embryonic MΦs have a very heterogeneous gene signature. These results also suggest that a percentage of EYFP$^+$CD45$^+$ cells, which appear to emerge from vessels in the mesenchyme, are distinct from MΦs.

Further analysis of the CD45$^+$non-MΦ population (Fig. 4E) revealed that it is composed of four fractions: Kit$^+$CD105$^-$/CD71$^-$ cells, which display a HC phenotype; Kit$^-$CD105$^+$/CD71$^+$ cells, with a more-enhanced mesenchymal phenotype; Kit$^+$CD105$^+$/CD71$^+$ cells that could be a transitional population; and Kit$^-$CD105$^-$/CD71$^-$, which are possibly more differentiated CD45$^+$ cells.

The presence of transitional populations co-expressing HC and mesenchymal markers is supported by the fact that 1 day later (E13.5; supplementary material Fig. S6) the CD45$^-$ population expressed mesenchymal markers at higher levels and the CD45$^+$ non-MΦ increased the expression of Kit, while still expressing mesenchymal markers at a higher level than at E12.5. This suggests that cells that co-expressed HC and mesenchymal genes are now downregulating some lineage-specific genes and transitioning to a more univocal phenotype. Accordingly, CD45$^+$MΦ cells significantly downregulated mesenchymal genes at E13.5.

The extra-embryonic origin of mesenchymal eVE-Cad$^+$-derived cells

Two possible origins of mesenchymal EYFP$^+$CD45$^+$non-MΦ cells can be postulated. We may observe endothelial-to-hematopoietic transition of hemogenic ECs in a direction that, in the mouse, is opposite to that of classical hematopoietic clusters, as reported during vascular remodeling of the vitelline artery (Zovein et al., 2010) but not further confirmed (Yokomizo et al., 2011). Conversely, these cells may originate from other VE-Cad-expressing cells in the embryo or extra-embryonic tissue, that reach the embryo mesenchyme by extravasation, where some maintain a hematopoietic phenotype, while others start to co-express mesenchymal markers. To elucidate this phenomenon, we performed Cre activation at different time points. Analysis of EYFP$^+$ cells was carried out at 12 h and 24 h after TAM injection to immediately follow the fate of labeled cells (Fig. 5A).

Labeling at E9.5 with analysis at E10-E10.5 revealed a lower number of EYFP$^+$CD41$^+$ cells in the YS (Fig. 5Bi-ii,F) compared with those detected when labeling at E8.5, whereas the number of EYFP$^+$CD45$^+$ was similar in both cases (Fig. 5Biii,F). Rare EYFP$^+$CD41$^+$ and EYFP$^+$CD45$^+$ cells were seen in the placenta at this time point (Fig. 5F; supplementary material Fig. S4C). Interestingly, EYFP$^+$CD41$^+$ and EYFP$^+$CD45$^+$ cells were hardly detected in either YS or placenta when injection was performed at E10.5 and analysis at E11-E11.5 (Fig. 5D,F; supplementary material Fig. S4C). This suggests that the hemogenic potency of extra-embryonic endothelium is restricted to a short time-window, starting at E8.5 or before, and progressively decreasing until E10.5, possibly ending shortly thereafter.

When induction was performed at E9.5 and E10.5, no EYFP$^+$CD41$^+$ or EYFP$^+$CD45$^+$ were observed in the mesenchyme of the embryo 24 h later (Fig. 5C,E). These EYFP$^+$ cells were seen in

Table 1. Summary of the contribution of eVE-Cadherin$^+$-derived cells (EYFP$^+$) to various lineages

Stage	Time of tamoxifen injection	Cell population	Tissue	Technique	Extent of contribution (percentage of EYFP$^+$ on total population)
E9.5	E8.5	Endothelial cells (CD31$^+$/VE-Cadherin$^+$)	Embryo	IF	80%
E9.5, E10.5 and E11.5	E8.5, E9.5 and E10.5	Somites (Pax3$^+$/MyoD$^+$, CD31$^-$)	Embryo	IF	No contribution
E12.5	E8.5	Hematopoietic cells (CD45$^+$)	Embryo, yolk sac and placenta	FACS	25.1% (embryo), 22.8% (yolk sac) and 1.5% (placenta)
E12.5	E8.5	'Mesoangioblasts' (CD45$^+$α-SMA$^+$ F4/80$^-$)	Embryo	FACS	52.1%
E12.5 and E15.5	E8.5	Smooth muscle (α-SMA$^+$/NG2$^+$ CD31$^-$)	Embryo	IF	1.1% (E12.5) and 2.3% (E15.5)
E12.5, E13.5 and E15.5	E8.5	Skeletal muscle (MyHC$^+$ CD31$^-$)	Embryo (total)	IF	0.9% (E12.5), 2% (E13.5) and 3.5% (E15.5)
E17.5 and P0	E8.5	Skeletal muscle (Desmin$^+$CD31$^-$)	Embryo (limb)	IF	0.5% (E17.5) and 1% (P0)
E13.5	E8.5	Myoblasts (Myogenin$^+$)	Embryo	IF	0.3%
E15.5	E8.5	Cardiomyocytes (MyHC$^+$ CD31$^-$)	Embryo	IF	No contribution
E15.5	E8.5	Endocardial cushion cells	Embryo	IF	~100%
E17.5	E8.5	Dermis (Collagen I$^+$ F4/80$^-$)	Embryo (limb)	IF	3.7%

EYFP, enhanced yellow fluorescent protein; FACS, fluorescence-activated cell sorting; IF, immunofluorescence.

Development (2014) 141, 1821-1834 doi:10.1242/dev.103242

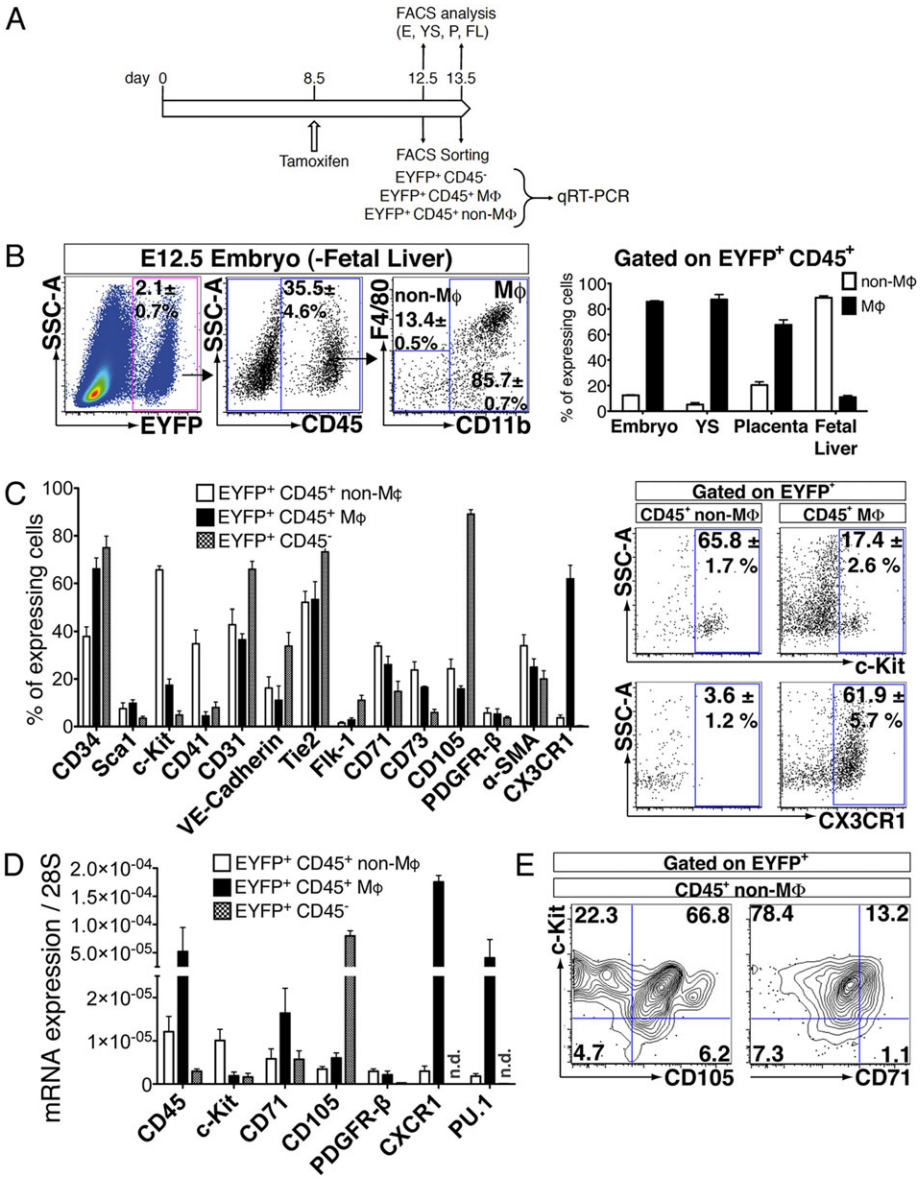

Fig. 4. Surface marker and gene expression characterization of eVE-Cad$^+$-derived non-MΦ cells. (A) Experimental scheme. (B) FACS analysis of E12.5 embryos, showing F4/80 and CD11b expression within the EYFP$^+$CD45$^+$ subset. A similar analysis was performed on YS, placenta and fetal liver. Graph shows the quantification of FACS analyses. *n*=3 independent experiments. (C) FACS analysis of E12.5 embryos, showing the expression of different markers within the three subsets of EYFP$^+$ cells defined as in B. Dot plots show the expression of two representative markers within the CD45$^+$non-MΦ and CD45$^+$ MΦ populations. *n*=3 independent experiments. (D) qRT-PCR analysis on freshly sorted cells from E12.5 embryos. The three subsets of EYFP$^+$ cells are defined as in B. Data are mean±s.e.m.; *n*=3 independent experiments. (E) FACS analysis of E12.5 embryos, showing the expression of Kit and two representative mesenchymal markers within the CD45$^+$non-MΦ population. *n*=3 independent experiments.

the embryo proper starting from E10.5 only when injection was performed at E8.5 (Fig. 3B,C; supplementary material Fig. S5), showing that at least 48 h are needed to allow EYFP$^+$ labeled cells at E8.5 to be found in the embryonic mesenchyme. With our induction protocol, expression of reporter genes is completed by 24 h (Park et al., 2007; Zovein et al., 2008). If EYFP$^+$CD45$^+$ and EYFP$^+$CD41$^+$ cells in the embryonic mesenchyme originated from hemogenic endothelium in the embryo proper we would have been able to detect them at E10.5-E11.5 by labeling VE-Cad$^+$ cells in the E9.5-E10.5 time-window, when embryonic endothelium starts to be hemogenic. This is not the case; thus, EYFP$^+$CD45$^+$ and EYFP$^+$CD41$^+$ cells in the embryonic mesenchyme likely originate from extra-embryonic endothelium (predominantly YS), and become labeled in the E8.5-E9.5 time-window, as YS hemogenic activity decreases later on, as described above. These results also imply that CD45$^+$α-SMA$^+$ cells in the mesenchyme have the same origin.

eVE-Cad$^+$-derived mesenchymal progenitors contribute to multiple mesodermal lineages during development

We have previously reported the isolation of multipotent vessel-associated stem cells in the embryo, MABs (Minasi et al., 2002). Our results suggest that MABs resemble the EYFP$^+$CD45$^+$α-SMA$^+$F4/80$^-$ cells observed in the embryo mesenchyme and may originate from an endothelial or hemogenic endothelial precursor, the EYFP$^+$CD45$^+$non-MΦ cells, which gives rise to both hematopoietic and mesenchymal lineages. To further investigate this hypothesis, we evaluated the contribution of eVE-Cad$^+$-derived cells to other mesodermal lineages (Fig. 6A).

At E12.5-E15.5 in the smooth muscle layer of large vessels we detected EYFP$^+$CD31$^-$ cells co-expressing α-SMA$^+$ or NG2$^+$, markers of the pericyte-smooth muscle lineage at those stages (1.1-2.3% of the total α-SMA$^+$ or NG2$^+$ peri-endothelial smooth muscle cells) (Fig. 6B, Table 1). EYFP$^+$NG2$^+$ cells found earlier at E10.5 were mostly CD31$^+$; at E11.5 they were mainly CD31$^-$ and in a perivascular location (supplementary material Fig. S5C).

We next examined the contribution of eVE-Cad$^+$-derived progenitors to the skeletal muscle lineage. At E9.5-E11.5, no EYFP$^+$ cells were found to colocalize with markers of somitic populations, such as Pax3, MyoD and Myf5 (supplementary material Fig. S7A), suggesting that eVE-Cad$^+$-derived progenitors do not give rise to myogenic cells within somites. Similar results were obtained when Cre recombinase was induced at later stages (supplementary

Development (2014) 141, 1821-1834 doi:10.1242/dev.103242

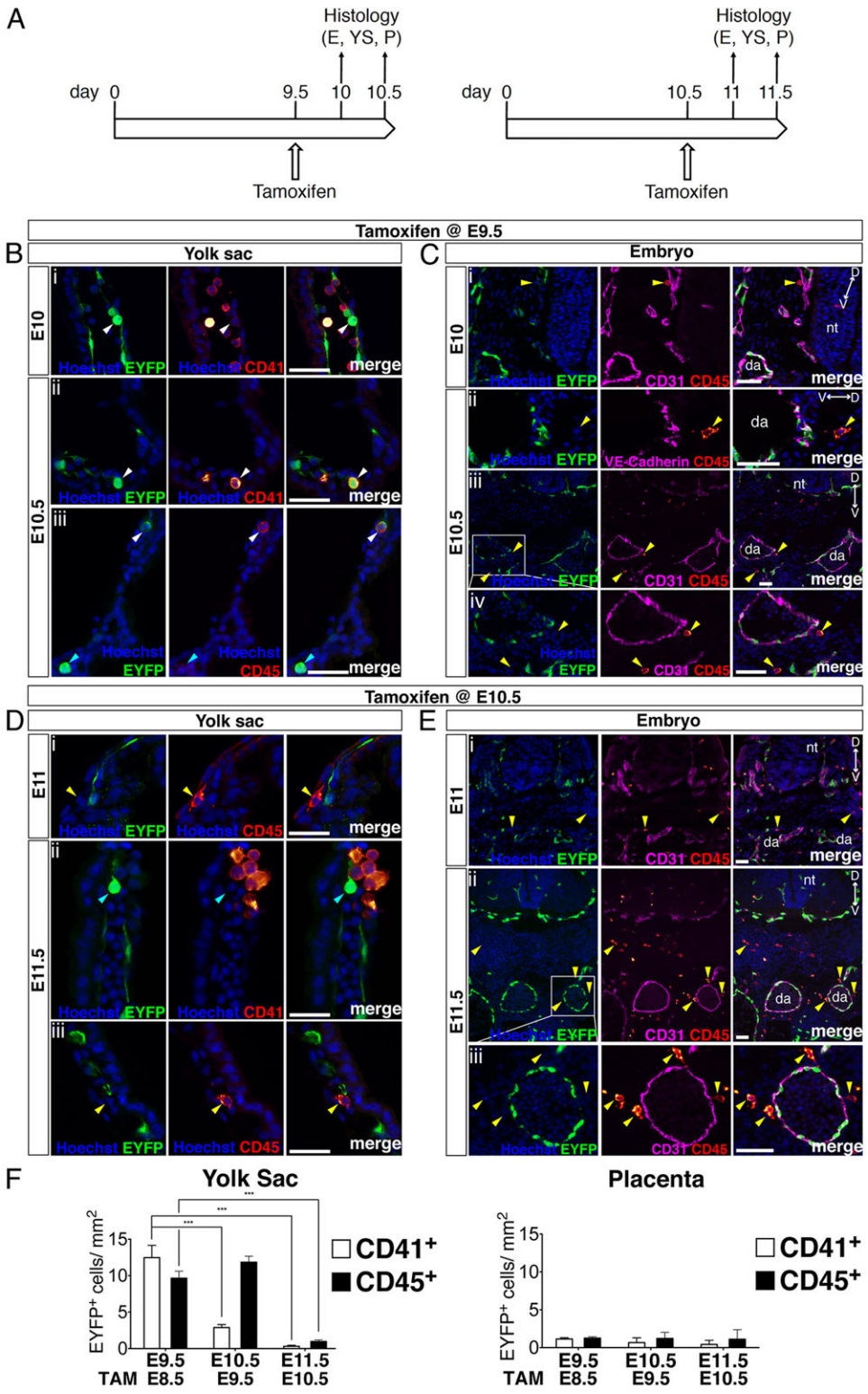

Fig. 5. The first wave of eVE-Cad$^+$-derived CD41$^+$ and CD45$^+$ cells in the mesenchyme originates from extra-embryonic hemogenic endothelium. (A) Experimental scheme. (B) Immunofluorescence (IF) using anti-EYFP and anti-CD41 (i-ii) or anti-CD45 (iii) on sections of E10 (i) and E10.5 (ii–iii) YS. White arrowheads indicate labeled CD41$^+$ and CD45$^+$ HCs; cyan arrowheads indicate a EYFP$^+$ CD45$^-$ HC. (C) IF using anti-EYFP, anti-CD45 and anti-CD31 (i,iii,iv) or anti-VE-Cadherin (ii) on sections of E10 (i) and E10.5 (ii-iv) embryos. Boxed area in iii is shown at higher magnification in iv. Yellow arrowheads indicate unlabeled CD45$^+$CD31$^-$ or CD45$^+$VE-Cadherin$^-$ HCs. (D) IF using anti-EYFP and anti-CD41 (ii) or anti-CD45 (i,iii) on sections of E11 (i) and E11.5 (ii,iii) YS. Yellow arrowheads indicate unlabeled CD45$^+$ HCs; cyan arrowheads indicate a EYFP$^+$CD41$^-$ HC. (E) IF using anti-EYFP, anti-CD45 and anti-CD31 on sections of E11 (i) and E11.5 (ii,iii) embryos. Boxed area in ii is shown at higher magnification in iii. Yellow arrowheads indicate unlabeled CD45$^+$ HCs. (F) Histological quantification of EYFP$^+$CD41$^+$ and EYFP$^+$CD45$^+$ cells in the YS and placenta at E9.5, E10.5 and E11.5 (tamoxifen induction 24 h before collection). ***P<0.001. Dorsoventral orientation is shown in C and E. da, dorsal aorta; nt, neural tube. Nuclei were stained with Hoechst. Scale bars: 50 μm.

material Fig. S7B). This was confirmed by qRT-PCR on sorted cells (supplementary material Fig. S7C). From E12.5 we observed EYFP$^+$CD31$^-$ mononucleated cells expressing skeletal myosin heavy chain (MyHC) (Fig. 6Cii-iv) or α-SMA (Fig. 6Ci), which at this stage is transiently expressed by skeletal myoblasts. In E12.5 embryos EYFP$^+$CD31$^-$MyHC$^+$/α-SMA$^+$ cells were still rare (Fig. 6Ci-ii,G). Importantly, at E12.5 and E13.5 we observed the presence of EYFP$^+$ myoblasts expressing myogenin (Fig. 6D), indicating that eVE-Cad$^+$-derived cells can undergo at least some of the steps of canonical skeletal myogenesis. EYFP$^+$MyHC$^+$ CD31$^-$ cells or EYFP$^+$Desmin$^+$CD31$^-$ were detected throughout the embryo until P0, the last time point of our analysis (Fig. 6C-F; supplementary material Fig. S8A and Movies 3, 4; Table 1). Fig. 6G summarizes the quantification of eVE-Cad$^+$-derived myogenic cells during development. qRT-PCR analysis on sorted EYFP$^+$ cells at different stages confirmed the expression of MyHC, desmin, MyoD, Pax3 and

Development (2014) 141, 1821-1834 doi:10.1242/dev.103242

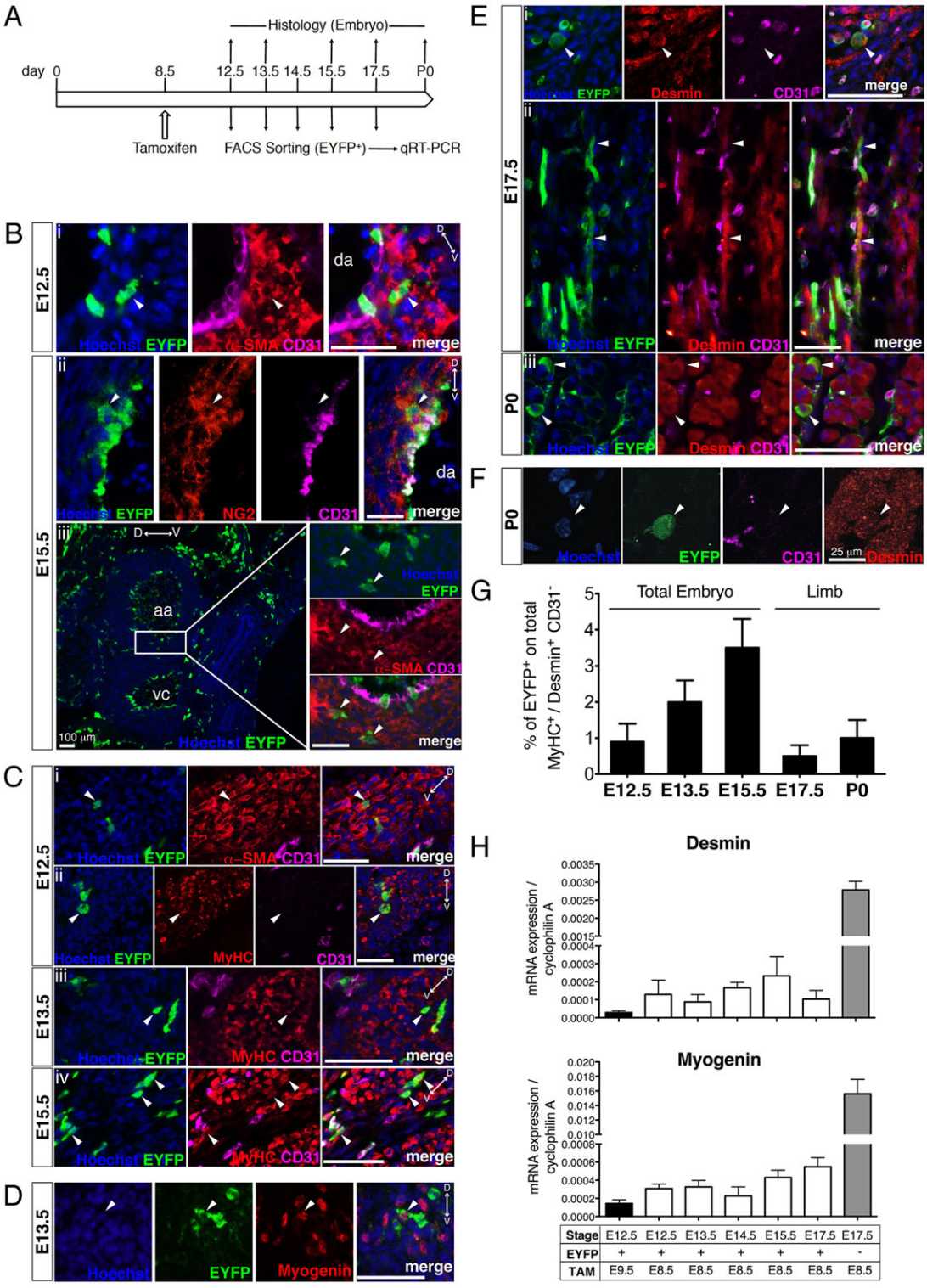

Fig. 6. eVE-Cad^{+}-derived cells contribute to smooth and skeletal muscle. (A) Experimental scheme. (B) Immunofluorescence (IF) using anti-EYFP, anti-CD31 and anti-α-SMA or anti-NG2 on transverse sections of E12.5 embryos (i) and E15.5 fetuses (ii,iii). Boxed area in iii is shown at higher magnification on the right. Arrowheads indicate EYFP^{+}α-SMA^{+}CD31^{-} or EYFP^{+}NG2^{+}CD31^{-} smooth muscle cells. (C) IF using anti-EYFP, anti-CD31 and anti-α-SMA (i) or anti-MyHC (ii) on transverse sections of E12.5 (i,ii), E13.5 (iii) and E15.5 (iv) embryos and fetuses. Arrowheads indicate EYFP^{+}α-SMA^{+}CD31^{-} or EYFP^{+}MyHC^{+}CD31^{-} single-nucleated myocytes/myofibers. (D) IF using anti-EYFP and anti-myogenin on transverse sections of a E13.5 embryo. Arrowhead indicates a EYFP^{+}Myogenin^{+} myocyte. (E) IF using anti-EYFP, anti-desmin and anti-CD31 on E17.5 (i,ii) or P0 (iii) hindlimb transverse (i) or longitudinal (ii) sections. Arrowheads indicate EYFP^{+}Desmin^{+}CD31^{-} myofibers. (F) Confocal IF imaging of P0 hindlimb transverse sections, using anti-EYFP, anti-desmin and anti-CD31. Arrowhead indicates a EYFP^{+}Desmin^{+}CD31^{-} myofiber. Scale bar: 25 μm. (G) Percentage of EYFP^{+} on total MyHC^{+}/Desmin^{+}CD31^{-} myocytes or myofibers at E12.5, E13.5, E15.5, E17.5 and P0. (H) qRT-PCR analysis on freshly sorted EYFP^{+} and EYFP^{-} cells at different stages and Cre induction times. Data are shown as mean±s.d.; *n*=2 independent experiments. Dorsoventral orientation is shown in each panel in B-D. da, dorsal aorta; aa, abdominal aorta; vc, vena cava. Nuclei were stained with Hoechst. Scale bars: 50 μm in B-E; 25 μm in F.

Development (2014) 141, 1821-1834 doi:10.1242/dev.103242

myogenin from E12.5 (Fig. 6H; supplementary material Fig. S8B). Interestingly, TAM injection at E9.5 resulted in a lower expression of all myogenic transcripts (Fig. 6H; supplementary material Fig. S8B). We concluded that some cells expressing VE-Cad at E8.5 and/or their progeny enter the embryonic myogenic lineage without going through somitic intermediates as part of their normal, unperturbed fate.

At E15.5 the heart displayed a high degree of EYFP labeling in the endocardium. However, no EYFP$^+$ cardiomyocytes were detected (supplementary material Fig. S9A). Almost all fibroblast-like endocardial cushion cells were EYFP$^+$CD31$^-$ (inset of supplementary material Fig. S9A), confirming that endocardial cushions arise from a subset of ECs that undergo endothelial-to-mesenchymal transition (Liebner et al., 2004).

At E17.5 the dermal layer surrounding the developing fingers contained a high number of EYFP$^+$ cells (supplementary material Fig. S9B). EYFP$^+$CD31$^-$Collagen I$^+$ cells and EYFP$^+$Collagen I$^+$F4/80$^-$ cells (supplementary material Fig. S9Biii,iv) were detected (3.7% of total Collagen I$^+$ cells, Table 1), indicating that eVE-Cad$^+$-derived cells, distinct from embryonic MΦs, had entered the dermal lineage. As expected, and partially described before by FACS (Fig. 4B), eVE-Cad$^+$ derived cells colonized fetal secondary hematopoietic organs (fetal liver, thymus and spleen) (supplementary material Fig. S9C). Taken together, these results confirm that eVE-Cad$^+$-derived cells contribute to several mesodermal lineages with variable, but significant, frequency.

eVE-Cad$^+$-derived CD45$^+$ cells, distinct from ECs and MΦs, display MAB features

To further verify whether eVE-Cad$^+$-derived cells resembled embryonic MABs after isolation and culture, we prepared aorta explant cultures from E9.5-E11.5 embryos 24 h after TAM induction, following the MAB isolation protocol (Fig. 7A; supplementary material Fig. S10A) (Tonlorenzi et al., 2007). After 1 week we observed the emergence of round, weakly adhering refractile cells, distinct from the populations of fibroblasts and floating HCs, and displaying MAB morphology. The majority of these cells were EYFP$^+$ and CD45$^+$ (Fig. 7B; supplementary material Fig. S10B). These data suggest that MABs originate from hemogenic endothelium, and, at least at early stages of *ex vivo* culture, display a hematopoietic phenotype.

We FACS isolated EYFP$^+$ cells from E12.5 embryos, a stage when CD45$^+$ cells in the mesenchyme are abundant (Fig. 7C). Isolated EYFP$^+$ cells were cultured in conditions suited for MABs and grew as a mixed population of spindle-shaped cells and small round-shaped cells (Fig. 7D).

eVE-Cad$^+$-derived cells were exposed to several differentiating stimuli. When treated with VEGF, they formed endothelial-like networks (Fig. 7Ei). TGFβ increased the number of α-SMA$^+$ cells with smooth muscle phenotype (80% versus 10% of untreated cells) (Fig. 7Eii). EYFP$^+$ cells expressed alkaline phosphatase (AP, a marker of pericytes and initial osteblastic differentiation) when treated with BMP2 (60-70% of AP$^+$ cells versus 5% of untreated)

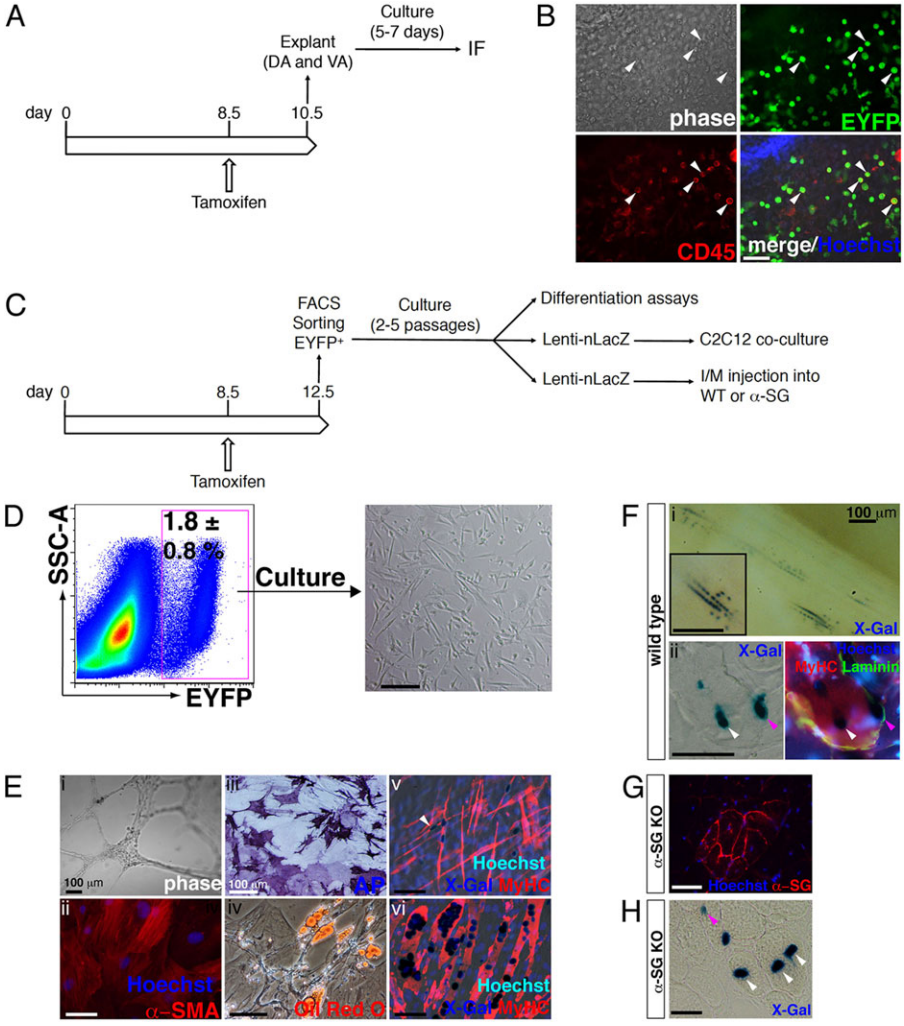

Fig. 7. eVE-Cad$^+$-derived cells resemble mesoangioblasts *in vitro*. (A) Experimental scheme of aorta and vitelline artery explants. (B) Immunofluorescence (IF) using anti-EYFP and anti-CD45. Arrowheads indicate EYFP$^+$ CD45$^+$ cells in the outgrowth. (C) Experimental scheme describing isolation of eVE-Cad$^+$-derived cells and downstream applications. (D) Representative dot plot showing FACS sorting of EYFP$^+$ cells from E12.5 embryos. A representative bright-field image of cultured EYFP$^+$ cells is shown on the right. (E) Isolated EYFP$^+$ cells were exposed to differentiating stimuli: (i) VEGF induces the formation of an endothelial network. (ii) TGFβ induces smooth muscle differentiation. IF using anti-α-SMA. (iii) Alkaline phosphatase (AP) staining of EYFP$^+$ cells after exposure to BMP2. (iv) Oil Red O staining of EYFP$^+$ cells induced to adipose differentiation. (v,vi) Myogenic differentiation of nLacZ-EYFP$^+$ cells in co-culture with C2C12 myoblasts was stopped after 3 (v) or 5 (vi) days. X-gal staining plus IF using anti-MyHC. nLacZ-EYFP$^+$ cells gave rise to X-gal$^+$/MyHC$^+$ myoblasts (arrowhead in v) and multinucleated myotubes (vi). (F) Intramuscular injection of nLacZ-EYFP$^+$ cells into CTX-damaged muscle of wild-type mice. (i) Whole-mount X-Gal staining showing superficial myofibers containing X-Gal$^+$ nuclei (inset at higher magnification). (ii) X-Gal staining plus IF using anti-laminin and anti-MyHC on muscle cross-sections. X-Gal$^+$ nuclei localize centrally (white arrowhead) or peripherally (purple arrowhead) inside myofibers. (G,H) Intramuscular injection of nLacZ-EYFP$^+$ cells into TA of α-SG KO mice. (G) IF using anti-α-SG on muscle cross-sections showing a cluster of regenerating α-SG$^+$ myofibers. (H) X-Gal staining on muscle cross-sections showing centrally (white arrowheads) or peripherally (purple arrowhead) localized X-Gal$^+$ nuclei inside myofibers. Scale bars: 100 μm.

Development (2014) 141, 1821-1834 doi:10.1242/dev.103242

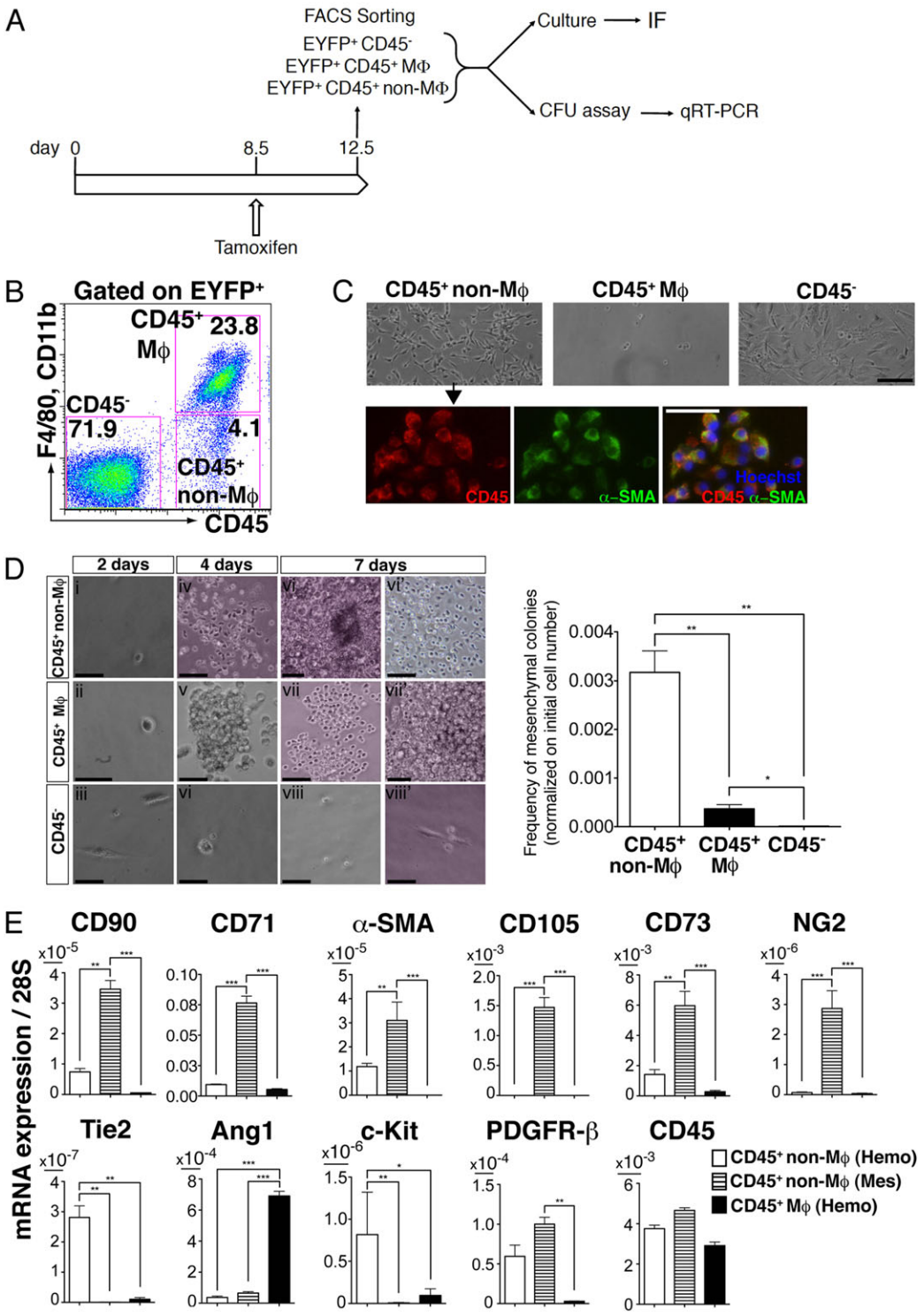

Fig. 8. eVE-Cad^{+}-derived CD45^{+}non-MΦ cells display mesenchymal features *in vitro*. (A) Experimental scheme. (B) Representative dot plot showing the gating strategy for FACS sorting. (C) Sorted cells were plated in MAB permissive conditions. Immunofluorescence (IF) shows co-expression of CD45 and α-SMA within the EYFP^{+}CD45^{+}non-MΦ subset. (D) Colony-forming cell (CFC) assay. Colonies were scored after 2, 4 or 7 days. EYFP^{+}CD45^{+}MΦ cells formed mostly hematopoietic colonies. EYFP^{+}CD45^{+}non-MΦ cells generated hematopoietic (vi) and mesenchymal-like colonies (iv,vi′). Graph shows the frequency of mesenchymal-like colonies in the different subsets, normalized to the initial cell number (four independent experiments). (E) Individual colonies from CFC assay (day 7) were picked and qRT-PCR was performed. Hemo, hematopoietic. Mes, mesenchymal-like. Data are mean±s.e.m.; *n*=3 independent experiments. **P*<0.05; ***P*<0.01; ****P*<0.001. Nuclei in IF were stained with Hoechst. Scale bars: 50 μm.

(Fig. 7Eiii). Culturing EYFP^{+} cells in adipogenic medium induced the appearance of adipocytes containing Oil Red O-positive fat droplets (Fig. 7Eiv).

When co-cultured with C2C12 murine myoblasts (after infection with a lentivirus directing expression of nLacZ), EYFP^{+} cells fused into multi-nucleated MyHC^{+} myotubes (Fig. 7Ev,vi). Single

Development (2014) 141, 1821-1834 doi:10.1242/dev.103242

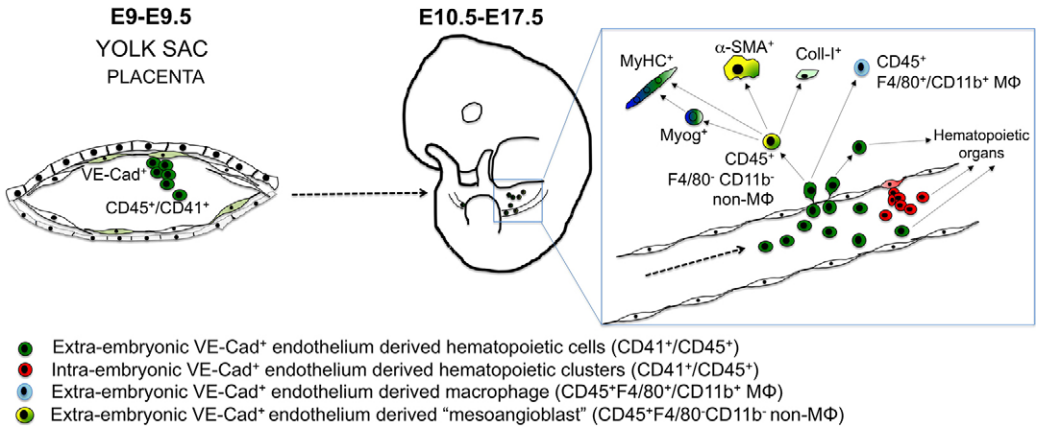

Fig. 9. Model of the generation of MABs from extra-embryonic hemogenic endothelium and their contribution to several mesodermal lineages. Extra-embryonic VE-Cad$^+$ hemogenic endothelial cells generate CD41$^+$/CD45$^+$ cells that migrate, probably through circulation, to the embryo proper, where they reach the mesenchyme by extravasation. Here, extra-embryonic-derived CD45$^+$F4/80$^-$CD11b$^-$ non-MΦ mesoangioblast cells contribute to several mesodermal lineages, including smooth muscle, skeletal muscle and dermis.

mononucleated MyHC$^+$β-Gal$^+$ cells were also detectable (arrow in Fig. 7Ev), indicating that eVE-Cad$^+$-derived cells were capable of direct myogenic differentiation. nLacZ-eVE-Cad$^+$-derived cells were injected into cardiotoxin-injured tibialis anterior (TA) muscles of wild-type mice. Donor-derived X-Gal$^+$ nuclei were found inside myofibers (Fig. 7Fi,ii), preferentially localized in a central position, typical of myonuclei inside regenerating myofibers (white arrow in Fig. 7Fii) but also peripherally and underneath the basal lamina (purple arrow in Fig. 7Fii). When injected into TA of immunosuppressed α-sarcoglycan (α-SG) KO mice, a model of limb-girdle muscular dystrophy, we observed the appearance of clusters of α-SG$^+$-regenerating myofibers (Fig. 7G,H). We conclude that eVE-Cad$^+$-derived cells are able to contribute to muscle regeneration *in vivo*.

The previous *in vivo* and *ex vivo* analyses showed that the EYFP$^+$ population in the embryo became more heterogeneous with time. To evaluate this heterogeneity *in vitro* and to discriminate which population carried MAB characteristics, we sorted the CD45$^+$MΦ (CD45$^+$F4/80$^+$CD11b$^+$) and the CD45$^+$nonMΦ (CD45$^+$F4/80$^-$CD11b$^-$) subsets (Fig. 8A,B).

In MAB culture conditions, only the CD45$^+$non-MΦ fraction gave rise to cells closely resembling embryonic MABs and co-expressing CD45 and α-SMA (Fig. 8C). CD45$^+$MΦ and CD45$^-$ cells grew poorly and the latter were generally bigger and heterogeneous in size and shape.

To identify the progeny of sorted cells at the single cell level, we performed a colony-forming cell (CFC) assay. Colonies started to form after 4 days, displaying different morphology (Fig. 8Div-vi). Only CD45$^+$ non-MΦ cells gave rise to mesenchymal-like colonies with high frequency (Fig. 8D, graph).

Single colony qRT-PCR (Fig. 8E) showed that mesenchymal markers such as α-SMA, PDGFRβ and CD90, CD105, CD73, CD71, NG2 were exclusively or significantly more expressed by CD45$^+$ non-MΦ mesenchymal colonies. Hematopoietic CD45$^+$ non-MΦ colonies, likely containing HCs, specifically expressed Tie2 and Kit. Hematopoietic CD45$^+$MΦ colonies, containing embryonic MΦs, expressed Ang1, but not Tie2, and did not express mesenchymal markers (Fig. 8E). The presence of CD45$^+$ non-MΦ-derived mixed hematopoietic and mesenchymal colonies is in agreement with the observation of a transitional population co-expressing HC and mesenchymal markers (Fig. 4E).

Taken together, these data suggest that cells bearing characteristics of cultured embryonic MABs originate from eVE-Cad$^+$-derived CD45$^+$ cells distinct from MΦs and can give rise to both hematopoietic cells and mesenchymal progenitor cells.

DISCUSSION

Endothelium has been shown to be a crossroad of several cell lineages during development. Recent work has shed light on the existence of hemogenic endothelium (Boisset et al., 2010; Kissa and Herbomel, 2010; Zovein et al., 2008), a specialized embryonic endothelial population that gives rise to the precursors of HSCs and therefore virtually to all the adult blood. Here, we show that at early developmental stages a population of progenitors with mesodermal potency, including HCs, originates from VE-Cad$^+$ ECs in the YS and in the placenta, in a very narrow temporal window (starting at E8.5 or before, progressively decreasing until E10.5 or shortly thereafter) (Fig. 9). Importantly, these extra-embryonic ECs are the only ones at this stage to give rise to HCs that are later found within the embryo mesenchyme. By activating Cre at different time points, we confirm that hemogenic endothelium in the embryo proper does not display this feature at early stages. Without a live imaging approach of whole intact mouse embryos, which is not currently possible to our knowledge, we can only speculate that they reach the mesenchyme through the circulation.

Clear evidence of the emergence of HSCs in the YS has not been provided (Wang and Wagers, 2011). E9-10 YS-derived cells can provide long-term contribution to adult hematopoiesis (Yoder et al., 1997), and by E11.5 YS contains true multilineage dHCs (Kumaravelu et al., 2002), thought to derive from hemangioblasts that migrate from the primitive streak (Huber et al., 2004). Yet, it has been suggested that from E8.25, CD41$^+$ definitive hematopoietic progenitors originate in the YS from cells bearing endothelial features (Li et al., 2005; Wang and Wagers, 2011).

Likewise, the placenta is a hematopoietic organ that can generate HSCs *de novo* and support their expansion without promoting differentiation, and it contains a large population of HSCs that arise slightly later than in the YS, concomitant with their appearance in the AGM region (Dzierzak and Robin, 2010; Rhodes et al., 2008). Several pieces of evidence suggest that some placental hematopoietic stem and progenitor cells are probably generated *in situ* by hemogenic endothelial cells (Zovein et al., 2008). We confirm the hematopoietic potency of extra-embryonic hemogenic endothelium and provide the first evidence that extra-embryonic and

Development (2014) 141, 1821-1834 doi:10.1242/dev.103242

embryonic hemogenic endothelia have different timings of activity, and possibly distinct biological characteristics.

The YS is also the source of embryonic MΦs, which first appear around E7.5 and infiltrate the embryo via the vasculature before E10.5, where they play important roles in tissue remodeling and organ development (Bertrand et al., 2005; Ovchinnikov, 2008; Schulz et al., 2012). We suggest that at least a subset of F4/80$^+$/CD11b$^+$ embryonic MΦs are generated from hemogenic endothelium. We also show the presence of another population, CD45$^+$non-MΦ eVE-Cad$^+$-derived cells in the mesenchyme that express α-SMA (Crawford et al., 2002) and other mesenchymal markers, such as CD71 (Tfrc), CD73 (Nt5e), CD105 (Eng) and PDGFRβ. Interestingly, CD105 expression has been correlated with YS bipotent progenitors that give rise to hematopoietic and endothelial progeny (Borges et al., 2013). In our case, CD45$^-$ cells express higher levels of CD105, whereas HCs are associated with a lower expression.

Several studies hinted at the possibility of the existence of a common precursor that may give rise to both endothelium and blood cells or pericytes/mesenchymal cells (DeRuiter et al., 1997; Yamashita et al., 2000). The embryonic dorsal aorta contains MABs, culture-defined progenitors that express hemo-angioblastic markers and are able, *in vitro* and in transplantation assays, to differentiate into most mesodermal tissues, including skeletal myofibers (Minasi et al., 2002). This is in agreement with the identification of mesenchymal stem/progenitor cells in the major hematopoietic sites during mouse development (Mendes, 2005). The distribution/tissue contribution of CD45$^+$non-MΦs eVE-Cad$^+$-derived cells overlaps with the one observed with transplantation of MAB cell lines, although we did not analyze clonal populations. Of importance, VE-Cad$^+$-derived cells express skeletal myogenic markers at RNA and protein levels. Although in many cases the frequency of labeling in mesodermal cells (smooth and skeletal muscle, dermis) was low, it was still significant and way above (minimum 10-fold) the level of any leakage observed at any stage, which only occurred in CD31$^+$/VE-Cadherin$^+$ cells (Table 1). In addition, we may underestimate the extent of the actual contribution of eVE-Cad$^+$ cells to the various lineages, because of the incomplete efficiency of Cre recombination.

Experiments on aorta explants and selected sorted populations showed that, at midgestation, eVE-Cad$^+$-derived cells give rise to endothelium, blood and mesenchymal cells in the embryo, and that a fraction of these cells maintained hematopoietic (CD45 and Kit) and mesenchymal markers. Furthermore, only the non-MΦ HCs subset of eVE-Cad$^+$-derived cells was able to give rise to cells closely resembling embryonic MABs and to generate with high efficiency colonies expressing mesenchymal genes. These data correlate with the *in vivo* presence of a transitional population of CD45$^+$non-MΦ eVE-Cad$^+$-derived cells co-expressing HC and mesenchymal markers that, during development, specify to either fate. These data therefore suggest that the CD45$^+$ non-MΦ eVE-Cad$^+$-derived cells bearing mesenchymal features are the *in vivo* counterparts of MABs, and indicate that the contribution of CD45$^+$MΦ eVE-Cad$^+$-derived cells to multilineage differentiation *in vivo* and *in vitro*, by direct differentiation or fusion, is marginal. This is in agreement with reports showing that CD11b$^+$ cells are not able to integrate into regenerating muscle fibers (Doyonnas et al., 2004; Ojima et al., 2004), whereas some myelomonocytic progenitors Kit$^+$ cells are. This is suggestive of a relationship between myelomonocytic cells and pericytes, MABs and other mesodermal precursors that will be extremely interesting to investigate.

In conclusion, we have demonstrated that extra-embryonic hemogenic endothelium generates, in a narrow developmental time window, the first wave of CD41$^+$ and CD45$^+$ HCs that disseminate the mesenchyme in the embryo proper. Most importantly, we suggest for the first time the developmental origin of embryonic MABs as a small subpopoulation of hemogenic endothelium-derived cells. Moreover, our data support the idea that the *in vitro* and *in vivo* myogenic and multi-lineage differentiation capabilities of MABs are not a cell culture or transplantation artefact, but rather an expression of a differentiation potential that also exists during normal development.

MATERIALS AND METHODS

Transgenic mice and CRE-ER^{T2} induction

Details of transgenic mice used in this work have been published previously: Cdh5-CREER^{T2} (Wang et al., 2010) and R26R-EYFP (Srinivas et al., 2001). All experiments conformed to Italian law and were performed under internal regulations for animal care and handling (IACUC 355 and 489).

Cre activity was induced by one single intra-peritoneal injection of pregnant females with 2 mg/25 g body weight of tamoxifen (TAM) (Sigma; 10 mg/ml in corn oil). Embryos were collected after natural overnight matings. Staging of E9-E11.5 embryos was performed by counting somite pairs (E9, 18-25 sp; E9.5, 26-30 sp; E10, 31-35 sp; E10.5, 36-40 sp; E11, 41-45 sp; E11.5, 46-50 sp). For E12.5 and later stages, fertilization was considered to take place at 6 a.m.

Immunofluorescence and antibodies

Immunofluorescence on frozen section of embryos and muscles was carried out as described previously (Brunelli et al., 2007). Details of the antibodies are provided in supplementary material Table S1. At least six embryos were analyzed for each condition (stage and TAM induction). Histological quantifications were carried out by counting at least 20 fields (20× and/or 40×) for each data point.

Quantitative real-time PCR

EYFP$^+$ cells sorted from embryos or picked from single colonies were processed using RNeasy Micro kit (Qiagen). Reverse transcription was performed using High-Capacity cDNA Reverse Transcription Kit (Applied Biosystems). Quantitative real-time PCR (qRT-PCR) analysis was performed using Mx3000P (Stratagene) or 7900HT FAST (Applied Biosystems) Real-Time PCR detection systems. cDNA samples were amplified using GoTaq qPCR Master Mix and Hot Start Polymerase (Promega). Primer sequences are provided in supplementary material Table S3. Data points were calculated in triplicate. CT values greater than 35 were considered negative signals. Quantification was carried out using the comparative C_T method. 28S or cyclophilin A were used as an internal control.

Flow cytometry

eVE-Cad$^+$-derived cells were isolated and processed as described previously (Biressi et al., 2007). For intracellular plus membrane FACS analysis, cells were first stained with membrane antibodies, then fixed and permeabilized with 0.1% saponin and 1% BSA in PBS.

Cell sorting was performed using the MoFLo system (Beckman Coulter). FACS analysis was carried out using LSR Fortessa or FacsCANTO (BD). At least 8-10 embryos, yolk sacs (YS), placentas or fetal livers were pooled for each experiment. Single stains and fluorescence minus one (FMO) controls were used to validate the position of the gates. Appropriate isotype controls were used. Dead cells were excluded by Hoechst 33258 (Invitrogen) or 7-aminoactinomycin D (Sigma) uptake. Data were analyzed using FlowJo software (TreeStar). Details on the antibodies are provided in supplementary material Table S2.

Explants, cell cultures and differentiation assays

Dissection and culture of explants of embryonic vessels were performed as described previously (Tonlorenzi et al., 2007). Sorted EYFP$^+$ cells were resuspended in DMEM with 20% FBS, bFGF (5 ng/ml) and β-mercaptoethanol (5 mg/ml) and spotted onto calf-skin collagen-coated dishes (sigma). Cells were kept in 3% oxygen.

Differentiation to smooth muscle, bone-like cells, adipocytes and endothelial networks was obtained as described previously (Tagliafico

et al., 2004; Balconi et al., 2000). Infection of sorted EYFP$^+$ cells with a lentiviral vector directing n*LacZ* expression (pRRL.sin.PPT.CMV.nLacZ.pre), *in vitro* myogenic differentiation and *in vivo* engraftment assay of at least 5×10^5 cells n*LacZ*-EYFP$^+$ cells in in TA muscles of C57/Bl6 or α-SGKO mice were performed as described previously (Dellavalle et al., 2007; Pessina et al., 2011).

Colony-forming cell (CFC) assay

Freshly sorted EYFP$^+$ cells from E12.5 embryos were plated in a methylcellulose-based medium (M3434, StemCell Technologies) according to the manufacturer's instructions. Colonies were evaluated at day 2, 4, 7 and 12. Mesenchymal-like colonies included adherent, spindle-shaped cells.

Image acquisition and manipulation

Fluorescent and phase-contrast images were taken using the following microscopes: Nikon Eclipse E600; Nikon ACT-1 acquisition software; Leica AF6000; Leica AF600 acquisition software; Leica TCS SP2 Laser Scanning Confocal; Zeiss LSM 780 Inverted Confocal. Images were assembled in panels using Adobe Photoshop CS4 and Adobe Illustrator CS4.

Statistical analysis

Data were analyzed with Microsoft Excel 12.2.3 and GraphPad Prism 5. Values are expressed as mean±s.e.m. or mean±s.d. To assess statistical significance, unpaired two-tailed Student's *t*-tests were used (where not specified, $*P<0.05$; $**P<0.01$; $***P<0.001$).

Acknowledgements

Part of this work was carried out in the ALEMBIC imaging center (San Raffaele Scientific Institute). We thank Elisabetta Dejana, Marella de Bruijn and Patrizia Rovere-Querini for comments and suggestions, and Mario Tirone for technical support.

Competing interests

The authors declare no competing financial interests.

Author contributions

E.A., S.B. and G.C. conceived and designed this research project. E.A., V.C. and L.C. performed experiments. All authors participated in analysis and discussion of the experimental data. E.A. and S.B. wrote the initial draft of the manuscript. All authors participated in editing and finalizing the manuscript.

Funding

This work was supported by the European Community's Seventh Framework Programme [241440 (ENDOSTEM to S.B.) and 223098 (OPTISTEM to G.C.)].

Supplementary material

Supplementary material available online at
http://dev.biologists.org/lookup/suppl/doi:10.1242/dev.103242/-/DC1

References

Balconi, G., Spagnuolo, R. and Dejana, E. (2000). Development of endothelial cell lines from embryonic stem cells: a tool for studying genetically manipulated endothelial cells in vitro. *Arterioscler. Thromb. Vasc. Biol.* **20**, 1443-1451.

Bertrand, J. Y., Jalil, A., Klaine, M., Jung, S., Cumano, A. and Godin, I. (2005). Three pathways to mature macrophages in the early mouse yolk sac. *Blood* **106**, 3004-3011.

Bertrand, J. Y., Chi, N. C., Santoso, B., Teng, S., Stainier, D. Y. R. and Traver, D. (2010). Haematopoietic stem cells derive directly from aortic endothelium during development. *Nature* **464**, 108-111.

Biressi, S., Tagliafico, E., Lamorte, G., Monteverde, S., Tenedini, E., Roncaglia, E., Ferrari, S., Ferrari, S., Cusella-De Angelis, M. G., Tajbakhsh, S. et al. (2007). Intrinsic phenotypic diversity of embryonic and fetal myoblasts is revealed by genome-wide gene expression analysis on purified cells. *Dev. Biol.* **304**, 633-651.

Boisset, J.-C., van Cappellen, W., Andrieu-Soler, C., Galjart, N., Dzierzak, E. and Robin, C. (2010). In vivo imaging of haematopoietic cells emerging from the mouse aortic endothelium. *Nature* **464**, 116-120.

Borges, L., Iacovino, M., Koyano-Nakagawa, N., Baik, J., Garry, D. J., Kyba, M. and Perlingeiro, R. C. R. (2013). Expression levels of endoglin distinctively identify hematopoietic and endothelial progeny at different stages of yolk sac hematopoiesis. *Stem Cells* **31**, 1893-1901.

Brunelli, S., Tagliafico, E., De Angelis, F. G., Tonlorenzi, R., Baesso, S., Ferrari, S., Niinobe, M., Yoshikawa, K., Schwartz, R. J., Bozzoni, I. et al. (2004). Msx2 and necdin combined activities are required for smooth muscle differentiation in mesoangioblast stem cells. *Circ. Res.* **94**, 1571-1578.

Brunelli, S., Sciorati, C., D'Antona, G., Innocenzi, A., Covarello, D., Galvez, B. G., Perrotta, C., Monopoli, A., Sanvito, F., Bottinelli, R. et al. (2007). Nitric oxide release combined with nonsteroidal antiinflammatory activity prevents muscular dystrophy pathology and enhances stem cell therapy. *Proc. Natl. Acad. Sci. U.S.A.* **104**, 264-269.

Chen, M. J., Li, Y., De Obaldia, M. E., Yang, Q., Yzaguirre, A. D., Yamada-Inagawa, T., Vink, C. S., Bhandoola, A., Dzierzak, E. and Speck, N. A. (2011). Erythroid/myeloid progenitors and hematopoietic stem cells originate from distinct populations of endothelial cells. *Cell Stem Cell* **9**, 541-552.

Costa, G., Mazan, A., Gandillet, A., Pearson, S., Lacaud, G. and Kouskoff, V. (2012). SOX7 regulates the expression of VE-cadherin in the haemogenic endothelium at the onset of haematopoietic development. *Development* **139**, 1587-1598.

Crawford, K., Flick, R., Close, L., Shelly, D., Paul, R., Bove, K., Kumar, A. and Lessard, J. (2002). Mice lacking skeletal muscle actin show reduced muscle strength and growth deficits and die during the neonatal period. *Mol. Cell. Biol.* **22**, 5887-5896.

Dellavalle, A., Sampaolesi, M., Tonlorenzi, R., Tagliafico, E., Sacchetti, B., Perani, L., Innocenzi, A., Galvez, B. G., Messina, G., Morosetti, R. et al. (2007). Pericytes of human skeletal muscle are myogenic precursors distinct from satellite cells. *Nat. Cell Biol.* **9**, 255-267.

Dellavalle, A., Maroli, G., Covarello, D., Azzoni, E., Innocenzi, A., Perani, L., Antonini, S., Sambasivan, R., Brunelli, S., Tajbakhsh, S. et al. (2011). Pericytes resident in postnatal skeletal muscle differentiate into muscle fibres and generate satellite cells. *Nat. Commun.* **2**, 499.

DeRuiter, M. C., Poelmann, R. E., VanMunsteren, J. C., Mironov, V., Markwald, R. R. and Gittenberger-de Groot, A. C. (1997). Embryonic endothelial cells transdifferentiate into mesenchymal cells expressing smooth muscle actins in vivo and in vitro. *Circ. Res.* **80**, 444-451.

Doyonnas, R., LaBarge, M. A., Sacco, A., Charlton, C. and Blau, H. M. (2004). Hematopoietic contribution to skeletal muscle regeneration by myelomonocytic precursors. *Proc. Natl. Acad. Sci. U.S.A.* **101**, 13507-13512.

Drake, C. J. and Fleming, P. A. (2000). Vasculogenesis in the day 6.5 to 9.5 mouse embryo. *Blood* **95**, 1671-1679.

Dzierzak, E. and Robin, C. (2010). Placenta as a source of hematopoietic stem cells. *Trends Mol. Med.* **16**, 361-367.

Huber, T. L., Kouskoff, V., Fehling, H. J., Palis, J. and Keller, G. (2004). Haemangioblast commitment is initiated in the primitive streak of the mouse embryo. *Nature* **432**, 625-630.

Kissa, K. and Herbomel, P. (2010). Blood stem cells emerge from aortic endothelium by a novel type of cell transition. *Nature* **464**, 112-115.

Kumaravelu, P., Hook, L., Morrison, A. M., Ure, J., Zhao, S., Zuyev, S., Ansell, J. and Medvinsky, A. (2002). Quantitative developmental anatomy of definitive haematopoietic stem cells/long-term repopulating units (HSC/RUs): role of the aorta-gonad-mesonephros (AGM) region and the yolk sac in colonisation of the mouse embryonic liver. *Development* **129**, 4891-4899.

Lancrin, C., Sroczynska, P., Stephenson, C., Allen, T., Kouskoff, V. and Lacaud, G. (2009). The haemangioblast generates haematopoietic cells through a haemogenic endothelium stage. *Nature* **457**, 892-895.

Li, W., Ferkowicz, M. J., Johnson, S. A., Shelley, W. C. and Yoder, M. C. (2005). Endothelial cells in the early murine yolk sac give rise to CD41-expressing hematopoietic cells. *Stem Cells Dev.* **14**, 44-54.

Liebner, S., Cattelino, A., Gallini, R., Rudini, N., Iurlaro, M., Piccolo, S. and Dejana, E. (2004). Beta-catenin is required for endothelial-mesenchymal transformation during heart cushion development in the mouse. *J. Cell Biol.* **166**, 359-367.

Medvinsky, A., Rybtsov, S. and Taoudi, S. (2011). Embryonic origin of the adult hematopoietic system: advances and questions. *Development* **138**, 1017-1031.

Mendes, S. C. (2005). Mesenchymal progenitor cells localize within hematopoietic sites throughout ontogeny. *Development* **132**, 1127-1136.

Minasi, M. G., Riminucci, M., De Angelis, L., Borello, U., Berarducci, B., Innocenzi, A., Caprioli, A., Sirabella, D., Baiocchi, M., De Maria, R. et al. (2002). The meso-angioblast: a multipotent, self-renewing cell that originates from the dorsal aorta and differentiates into most mesodermal tissues. *Development* **129**, 2773-2783.

Mitchell, K. J., Pannerec, A., Cadot, B., Parlakian, A., Besson, V., Gomes, E. R., Marazzi, G. and Sassoon, D. A. (2010). Identification and characterization of a non-satellite cell muscle resident progenitor during postnatal development. *Nat. Cell Biol.* **12**, 257-266.

Ojima, K., Uezumi, A., Miyoshi, H., Masuda, S., Morita, Y., Fukase, A., Hattori, A., Nakauchi, H., Miyagoe-Suzuki, Y. and Takeda, S.-i. (2004). Mac-1(low) early myeloid cells in the bone marrow-derived SP fraction migrate into injured skeletal muscle and participate in muscle regeneration. *Biochem. Biophys. Res. Commun.* **321**, 1050-1061.

Ovchinnikov, D. A. (2008). Macrophages in the embryo and beyond: much more than just giant phagocytes. *Genesis* **46**, 447-462.
Park, E. J., Sun, X., Nichol, P., Saijoh, Y., Martin, J. F. and Moon, A. M. (2007). System for tamoxifen-inducible expression of cre-recombinase from the Foxa2 locus in mice. *Dev. Dyn.* **237**, 447-453.
Pessina, P., Conti, V., Tonlorenzi, R., Touvier, T., Meneveri, R., Cossu, G. and Brunelli, S. (2011). Necdin enhances muscle reconstitution of dystrophic muscle by vessel-associated progenitors, by promoting cell survival and myogenic differentiation. *Cell Death Differ.* **19**, 827-838.
Pucci, F., Venneri, M. A., Biziato, D., Nonis, A., Moi, D., Sica, A., Di Serio, C., Naldini, L. and De Palma, M. (2009). A distinguishing gene signature shared by tumor-infiltrating Tie2-expressing monocytes, blood "resident" monocytes, and embryonic macrophages suggests common functions and developmental relationships. *Blood* **114**, 901-914.
Rhodes, K. E., Gekas, C., Wang, Y., Lux, C. T., Francis, C. S., Chan, D. N., Conway, S., Orkin, S. H., Yoder, M. C. and Mikkola, H. K. A. (2008). The emergence of hematopoietic stem cells is initiated in the placental vasculature in the absence of circulation. *Cell Stem Cell* **2**, 252-263.
Russo, V., Zhou, D., Sartirana, C., Rovere, P., Villa, A., Rossini, S., Traversari, C. and Bordignon, C. (2000). Acquisition of intact allogeneic human leukocyte antigen molecules by human dendritic cells. *Blood* **95**, 3473-3477.
Sampaolesi, M., Torrente, Y., Innocenzi, A., Tonlorenzi, R., D'Antona, G., Pellegrino, M. A., Barresi, R., Bresolin, N., De Angelis, M. G. C., Campbell, K. P. et al. (2003). Cell therapy of alpha-sarcoglycan null dystrophic mice through intra-arterial delivery of mesoangioblasts. *Science* **301**, 487-492.
Schulz, C., Perdiguero, E. G., Chorro, L., Szabo-Rogers, H., Cagnard, N., Kierdorf, K., Prinz, M., Wu, B., Jacobsen, S. E. W., Pollard, J. W. et al. (2012). A lineage of myeloid cells independent of Myb and hematopoietic stem cells. *Science* **336**, 86-90.
Srinivas, S., Watanabe, T., Lin, C.-S., William, C. M., Tanabe, Y., Jessell, T. M. and Costantini, F. (2001). Cre reporter strains produced by targeted insertion of EYFP and ECFP into the ROSA26 locus. *BMC Dev. Biol.* **1**, 4.
Tagliafico, E., Brunelli, S., Bergamaschi, A., De Angelis, L., Scardigli, R., Galli, D., Battini, R., Bianco, P., Ferrari, S. and Cossu, G. (2004). TGFbeta/BMP activate the smooth muscle/bone differentiation programs in mesoangioblasts. *J. Cell Sci.* **117**, 4377-4388.
Tonlorenzi, R., Dellavalle, A., Schnapp, E., Cossu, G. and Sampaolesi, M. (2007). Isolation and characterization of mesoangioblasts from mouse, dog, and human tissues. *Curr. Protoc. Stem Cell Biol.* Chapter 2, Unit 2B 1.
Wang, L. D. and Wagers, A. J. (2011). Dynamic niches in the origination and differentiation of haematopoietic stem cells. *Nat. Rev. Mol. Cell Biol.* **12**, 643-655.
Wang, Y., Nakayama, M., Pitulescu, M. E., Schmidt, T. S., Bochenek, M. L., Sakakibara, A., Adams, S., Davy, A., Deutsch, U., Lüthi, U. et al. (2010). Ephrin-B2 controls VEGF-induced angiogenesis and lymphangiogenesis. *Nature* **465**, 483-486.
Yamashita, J., Itoh, H., Hirashima, M., Ogawa, M., Nishikawa, S., Yurugi, T., Naito, M., Nakao, K. and Nishikawa, S.-I. (2000). Flk1-positive cells derived from embryonic stem cells serve as vascular progenitors. *Nature* **408**, 92-96.
Yoder, M. C., Hiatt, K. and Mukherjee, P. (1997). In vivo repopulating hematopoietic stem cells are present in the murine yolk sac at day 9.0 postcoitus. *Proc. Natl. Acad. Sci. U.S.A.* **94**, 6776-6780.
Yokomizo, T., Ng, C. E. L., Osato, M. and Dzierzak, E. (2011). Three-dimensional imaging of whole midgestation murine embryos shows an intravascular localization for all hematopoietic clusters. *Blood* **117**, 6132-6134.
Zovein, A. C., Hofmann, J. J., Lynch, M., French, W. J., Turlo, K. A., Yang, Y., Becker, M. S., Zanetta, L., Dejana, E., Gasson, J. C. et al. (2008). Fate tracing reveals the endothelial origin of hematopoietic stem cells. *Cell Stem Cell* **3**, 625-636.
Zovein, A. C., Turlo, K. A., Ponec, R. M., Lynch, M. R., Chen, K. C., Hofmann, J. J., Cox, T. C., Gasson, J. C. and Iruela-Arispe, M. L. (2010). Vascular remodeling of the vitelline artery initiates extravascular emergence of hematopoietic clusters. *Blood* **116**, 3435-3444.